

X-Ray Photoelectron Spectroscopic Study of Alternately Layered Zirconium and Hafnium Phosphonate Thin Films on Silicon Substrates

Yasushi Umemura,^{*} Akihiko Yamagishi,[†] and Ken-ichi Tanaka^{††}

Department of Chemistry, National Defense Academy, Yokosuka, Kanagawa 239

[†]Division of Biological Sciences, Graduate School of Science, Hokkaido University, Sapporo 060

^{††}Institute of Solid State Physics, The University of Tokyo, Roppongi, Minato-ku, Tokyo 106

(Received April 14, 1997)

Multilayer films of alternately layered zirconium and hafnium phosphonates on silicon substrates were prepared and characterized by X-ray photoelectron spectroscopy. It is revealed that the multilayer film is built up layer-by-layer in the repeated order of a zirconium phosphonate layer and a hafnium phosphonate layer. The relative peak intensity of the Zr 3d line to the Hf 4d_{5/2} line in the photoelectron spectra of the film takes a lower value as the take-off angle between the surface normal and the detector (α) increases. The mean free path of a photoelectron with an energy of ca. 1000 eV was estimated to be 70–90 Å in the film by analyzing the α dependence of the relative peak intensities.

Self-assembling monolayers on substrates have been studied by many workers in order to use thin films as, for instance, chemically modified electrodes,^{1–5} molecular rectifiers,⁶ chemical sensors,⁷ and photoresists.^{8–10} Recently, a desire to design films at the molecular level or to control the properties of the films makes self-assembling multilayer films more attractive than monolayer films. The concept concerning the formation of self-assembling multilayer films by using chemical bond was first proposed by Netzer and Sagiv,¹¹ and rapid and striking progress has been made in this field since the publication of a report by Lee and his co-workers.^{12,13} Various kinds of chemical bonds are employed to fabricate self-assembling multilayer films, such as covalent bonds,^{11,14} ionic bonds,^{15–19} and coordination bonds.^{12,13,20–27}

Although X-ray photoelectron spectroscopy (XPS) is one of the most useful techniques for the characterization of a thin film on a solid surface, it is difficult to obtain quantitative information about an element composition in the film from the peak intensity in the spectrum.

The chemical and physical properties of zirconium and hafnium are so close that it is very difficult to control the arrangement of zirconium and hafnium atoms at the molecular level. In this work, we prepared films of alternately layered zirconium and hafnium phosphonates on silicon substrates according to a method by Lee et al.,^{12,13} and analyzed the relative peak intensities of the zirconium and hafnium lines in the X-ray photoelectron spectra of the films.²³ Akhter and his co-workers²⁷ characterized a trilayered film of Zr, Y, and Hf phosphonates by XPS; there was a small ambiguity in their characterization about the layered structure and estimation of the mean free path of the photoelectron. We also determined the mean free path of a photoelectron (ca. 1000 eV) in zirconium and hafnium phosphonate multilayer films by analyzing the take-off angle dependence of the relative

peak intensities.

Experimental

We prepared zirconium and hafnium phosphonate multilayer films on silicon surfaces by a modified method²³ according to the literature.¹³ A bridging agent to bind the zirconium ion and hafnium ion, 1,10-decanediylbis(phosphonic acid) [H₂O₃P(CH₂)₁₀PO₃H₂] (DBPA), was synthesized from 1,10-dibromodecane and triethyl phosphite using the Michaelis–Arbuzov reaction; also, an anchoring agent, 3-(hydroxydimethylsilyl)propylphosphonic acid [HO-(CH₃)₂Si(CH₂)₃PO₃H₂] (**1**), was prepared by reacting 1,3-bis-(3-chloropropyl)-1,1,3,3-tetramethyldisiloxane with P(OC₂H₅)₃. Metal ions were provided as 5 mmol dm^{−3} aqueous solutions of zirconium(IV) dichloride oxide octahydrate or hafnium(IV) dichloride oxide octahydrate (reagent grade). Single-crystal silicon wafers with polished (111) faces were employed as substrates, and the wafers were washed with trichloroethylene for 5 min, propane-2-ol for 10 min, and finally distilled water for 20 min before use. Anchoring was performed by immersing the silicon wafer for 4 months in a 5 mmol dm^{−3} aqueous solution of **1** at pH 7. A film was formed by placing the anchored wafer for 30–60 min in 5 mmol dm^{−3} aqueous solutions of ZrOCl₂, DBPA, HfOCl₂, DBPA, ZrOCl₂, one after another.

X-ray photoelectron spectra were recorded by using Mg K α radiation (1253.6 eV) as the X-ray source. The binding energies were corrected so that the peak position of the single crystal silicon 2p line was set at 99.15 eV as the standard. When the Si 2p peak couldn't be detected for a sample wafer with a thick multilayer film, we measured the edge of the wafer where the film had been removed mechanically.

Metal phosphonate powder of Zr–DBP (or Hf–DBP) was obtained by mixing stoichiometric amounts of an aqueous ZrOCl₂ solution (or an aqueous HfOCl₂ solution) and an aqueous DBPA solution to form a white precipitate. The precipitate was washed with a large amount of water and dried under ambient atmosphere. The X-ray photoelectron spectra of the bulk samples were measured by putting them on Scotch tape.

Results and Discussion

Figure 1 shows the X-ray photoelectron spectra of a film comprising one zirconium layer and one hafnium layer on a silicon wafer, which is denoted by $\text{Si}-(\text{Zr}-\text{Hf})_n$ ($n=1$). It was prepared by immersing the anchored silicon wafer in an aqueous ZrOCl_2 solution first, then in an aqueous DBPA solution, and finally in an aqueous HfOCl_2 solution. The spectra of $\text{Si}-(\text{Zr}-\text{Hf})_1$ in Fig. 1 were recorded at various take-off angles (α) between the surface normal and the detector (see an inset of the figure). The spectrum at $\alpha=14.0^\circ$ (Fig. 1,

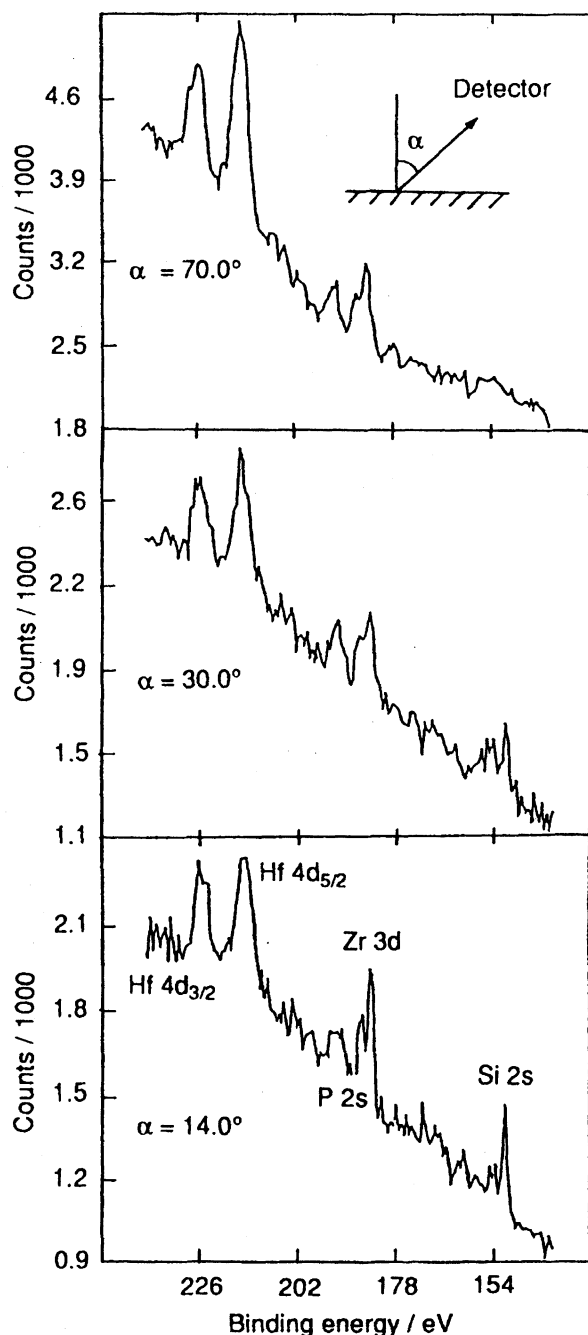


Fig. 1. X-Ray photoelectron spectra for the zirconium and hafnium phosphonate film $\text{Si}-(\text{Zr}-\text{Hf})_1$ at take-off angle $\alpha=14.0^\circ$ (lower), $\alpha=30.0^\circ$ (middle), and $\alpha=70.0^\circ$ (upper).

lower) gives several peaks, assigned from the lower binding energy side, to lines of Si 2s (153 eV), Zr 3d that splits to $3d_{5/2}$ (183 eV) and $3d_{3/2}$ (185 eV), P 2s (191 eV), Hf $4d_{5/2}$ (214 eV), and Hf $4d_{3/2}$ (225 eV), as shown in the figure.

The Si 2s peak is attributed to the silicon atoms of the substrate, and the P 2s peak to the phosphorus atoms of the anchoring agent 1 and the bridging ligand DBP in the film. The Si 2s peak decreases in intensity as α increases until it disappears at $\alpha=70.0^\circ$, whereas the P 2s peak remains in the spectrum at any take-off angle. It is well known that the contribution of electrons emitted from a deep part from the surface to the peak intensity decreases along with an increase in α . Based on this, the silicon atoms exist in the deep part from the surface of the sample, though the phosphorus atoms lie in the surface. Hence, the film covers the surface of the silicon substrate without any uncoated areas. The relative peak intensities of the Zr 3d lines to the Hf $4d_{5/2}$ and $4d_{3/2}$ lines decrease in going from $\alpha=14.0^\circ$ to $\alpha=70.0^\circ$, which indicates that the zirconium layer lies in a deeper part of the film than the hafnium layer.

Multilayer films of $\text{Si}-(\text{Zr}-\text{Hf})_n$ ($n=1-10$) were prepared by the repeated deposition of DBPA, Zr^{4+} ion, DBPA, and Hf^{4+} ion, as described in the experimental section. The XPS data of the films were collected with the take-off angle fixed at $\alpha=45.0^\circ$. The relative peak-area intensities of the Zr 3d ($3d_{5/2}$ and $3d_{3/2}$) peaks to the Hf $4d_{5/2}$ peak ($R_{(\text{Zr}/\text{Hf})}$) are plotted as a function of the number of layers in Fig. 2, together with the peak positions of Zr $3d_{5/2}$, Zr $3d_{3/2}$, and Hf $4d_{5/2}$. $R_{(\text{Zr}/\text{Hf})}$ takes higher values when the zirconium ion layer is at the top of the film than when the hafnium ion layer is at the top (Fig. 2, lower). As a whole, the value of $R_{(\text{Zr}/\text{Hf})}$ changes periodically from $\text{Si}-(\text{Zr}-\text{Hf})_1$ to $\text{Si}-(\text{Zr}-\text{Hf})_{10}$. This result leads to the view that the multilayers are built up exactly in a layer-by-layer way with no occurrence of collapse.

The peak position of the Zr $3d_{5/2}$ line shifts to a higher binding-energy side as the number of layers increases, and the positions of the Zr $3d_{3/2}$ and Hf $4d_{5/2}$ lines show a similar tendency (Fig. 2, middle and upper). The slopes of the shifts for these three peaks are almost the same, and, in addition, the position of the P 2s peak also shifts in the same way as those of the peaks due to the metal ions. From these experimental data, the shifts of the peaks result not from any change in the electronic structures of the atoms in the film, but from the effect of positive charging on the film during the XPS measurement. In turn, the fact that the shifts of the peak positions by charging the film have a good linear correlation with the film thickness supports the exact formation of a film layer-by-layer.

In order to determine the mean free path of a photoelectron in zirconium and hafnium phosphonate films, the photoelectron spectra of the films were recorded at various take-off angles; also, the α dependence of the peak intensity was analyzed. The α dependence of $R_{(\text{Zr}/\text{Hf})}$ for the film $\text{Si}-(\text{Zr}-\text{Hf})_2$ is given as a function of $\cos \alpha$ in Fig. 3, in which $R_{(\text{Zr}/\text{Hf})}$ exhibits a higher value with an increase in $\cos \alpha$.

A possibility that an electron travels straight for a distance l without any scattering in a dense material is given by

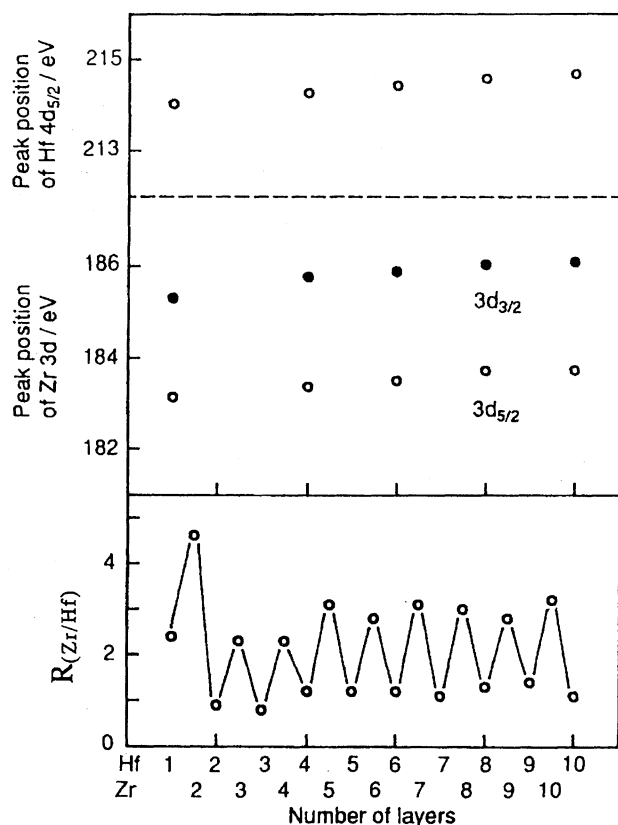


Fig. 2. The relative peak area intensity of the Zr 3d ($3d_{5/2}$ and $3d_{3/2}$) to the Hf $4d_{5/2}$ (lower) and the peak positions of the Zr $3d_{5/2}$, the Zr $3d_{3/2}$ (middle), and the Hf $4d_{5/2}$ (upper) as a function of the number of layers.

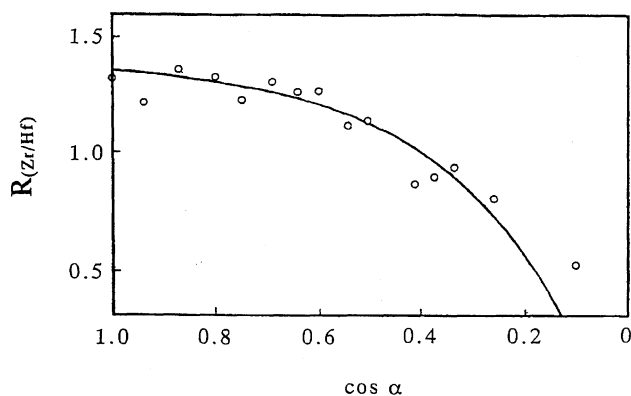


Fig. 3. The dependence of the relative peak intensity of the Zr 3d to the Hf $4d_{5/2}$ on the take-off angle α for the film of $\text{Si}-(\text{Zr}-\text{Hf})_2$. The solid line denotes the result of the best fit of the equation (see text).

$$\exp(-l/\lambda),$$

where λ is the mean-free path of the electron.²⁸⁾ From this, we can obtain an equation for $R_{(\text{Zr}/\text{Hf})}$ by summing the contribution of every layer to the peak intensity in the spectrum over the entire structure,

$$R_{(\text{Zr}/\text{Hf})} = \frac{\sum i_{\text{Zn}} \cdot \exp(-l_n^{\text{Zn}}/\lambda)}{\sum i_{\text{Hf}} \cdot \exp(-l_n^{\text{Hf}}/\lambda)},$$

$$l_n = \text{dep}_n / \cos \alpha.$$

Here, i_{Zn} and i_{Hf} are the relative electron yields for the Zr 3d and Hf $4d_{5/2}$ lines, l_n is a distance that an electron travels from the n -th layer to the surface of the film, and dep_n is a depth of the n -th layer from the surface of the film. Here, we assume the following three things: (1) The film is isotropic though the DBP molecules in the film are oriented. (2) The distances between the substrate and the zirconium-ion first layer and between the zirconium-ion layer and the hafnium-ion layer are set at 5.5 and 17.3 Å, respectively. The latter value is taken from the results of an X-ray diffraction analysis for bulk zirconium-DBP.²⁹⁾ (3) A photoelectron is scattered elastically on the surface of the substrate, the contribution of which is introduced into our calculation by being taken as mirror images of the layers. This is graphically illustrated in Fig. 4.

We carried out a fitting analysis for the experimental data of the film of $\text{Si}-(\text{Zr}-\text{Hf})_2$ by using the equation described above, treating the ratio $i_{\text{Zn}}/i_{\text{Hf}}$ and the photoelectron mean free path (λ) as parameters. The best fit is obtained when $i_{\text{Zn}}/i_{\text{Hf}} = 1.5$ and $\lambda = 85$ Å; the result is drawn in Fig. 3 as a solid line. According to the literature,^{30,31)} the ratio $i_{\text{Zn}}/i_{\text{Hf}}$ has been estimated to be 1.2. However, the ratio $i_{\text{Zn}}/i_{\text{Hf}}$ can be acquired from the photoelectron spectra of bulk Zr-DBP and bulk Hf-DBP by a comparison with the peak area of the P 2s line in each spectrum; the obtained ratio is 1.5. This agrees with the value from the fitting analysis, which implies the validity of the fitting analysis. A similar fitting analysis for data of the film $\text{Si}-(\text{Zr}-\text{Hf})_9$ gives the results $i_{\text{Zn}}/i_{\text{Hf}} = 1.4$ and $\lambda = 75$ Å. Considering the quality of the data, it is proper that the mean-free path of a photoelectron with an energy of ca. 1000 eV is 70–90 Å in a multilayer film. The photoelectron

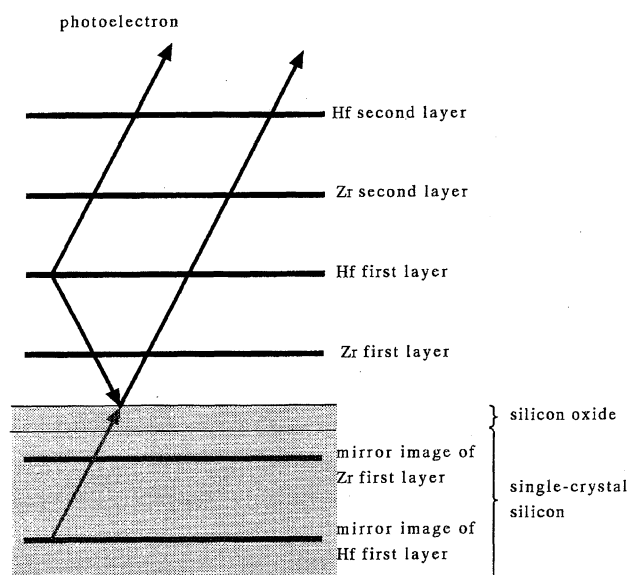


Fig. 4. The schematic view of the multilayer film, the substrate, and the mirror images of the layers. An electron that is emitted from a layer and scattered elastically on the substrate is treated as an electron emitted from the mirror image of the corresponding layer.

mean-free paths in zinc phosphonate films were estimated from XPS data;²⁴⁾ the values are 60 and 136 Å for zinc and phosphorus, respectively, which are slightly different from the value obtained in this work.

The value of the photoelectron mean-free path in the film corresponds to the thickness of 4–5 layers. This is consistent with the fact that the Si 2s line due to silicon atoms of the substrate disappears in the spectrum of the film Si-(Zr-Hf)₂ at a take-off angle (α) of 45°. Additionally, it is pointed out that $R_{(Zr/Hf)}$ shows a higher value from the Hf first layer to the Zr second layer in Fig. 2 (lower). This irregularity is well explained by the photoelectron mean-free path in the film and the elastic scattering of photoelectrons on the surface of the substrate. The mirror image of the Zr first layer contributes largely to the Zr peak intensity in the XPS data of the film with a small number of layers, and the contribution of the mirror image of the Zr first layer decreases exponentially in the XPS data as the film becomes thicker. Thus, $R_{(Zr/Hf)}$ appears to show a higher value for a film with 2 or 3 layers.

According to grazing-angle X-ray diffraction measurements by Zeppenfeld and his co-workers, the density of a Hf-DBP multilayer film is only ca. 75% of the corresponding

Table 1. Half Widths of Zr 3d Lines and Relative Peak Intensities of Zr 3d_{5/2} Line to Zr 3d_{3/2} Line in XPS for Si-(Zr-Hf)_n (n=4, 6, 8, 10) Films and Zr-DBP Bulk

	Half width (eV)		Relative peak intensity
	3d _{5/2}	3d _{3/2}	
Si-(Zr-Hf) _n			
n = 4	2.0	1.9	1.6
6	1.9	2.0	1.4
8	2.0	2.1	1.6
10	1.9	2.0	1.4
Zr-DBP	2.6	2.0	2.2

bulk material. This indicates that the structure of a Hf-DBP film is different from those accepted for bulk Hf-DBP or Zr-DBP based on the α -Zr(O₃POH)₂ structure.²⁹⁾ Figure 5 compares the contours of the Zr 3d lines between the film of Si-(Zr-Hf)₄ and the bulk Zr-DBP. As the result of a curve-fitting analysis, the half width of the Zr 3d_{5/2} line for the bulk (2.6 eV) is broader than that for the film (2.0 eV) and the relative peak intensity of the 3d_{5/2} line to the 3d_{3/2} line for the bulk (2.2) is larger than that for the film (1.6), which indicates that the electronic structures of the zirconium atoms in the bulk and in the film are different. Almost the same contours of the Zr 3d lines are given in the spectra for the films of Si-(Zr-Hf)_n (n = 4, 6, 8, 10). Table 1 lists the half widths of the Zr 3d lines and the relative peak intensities of the 3d_{5/2} line to the 3d_{3/2} line for the films Si-(Zr-Hf)_n (n = 4, 6, 8, 10) and for the bulk Zr-DBP. Those results suggest that the film takes a characteristic structure that is independent of the film thickness and different from the bulk structure.

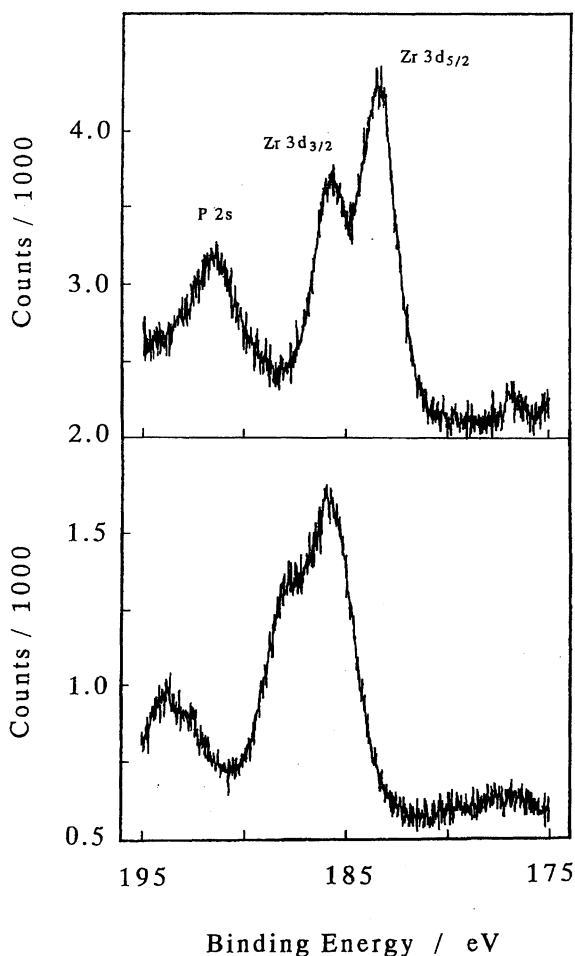


Fig. 5. The X-ray photoelectron spectra of the Zr 3d_{5/2}, 3d_{3/2}, and the P 2s lines for the multilayer film Si-(Zr-Hf)₄ (upper) and the Zr-DBP powder (lower).

References

- 1) T. T.-T. Li and M. J. Weaver, *J. Am. Chem. Soc.*, **106**, 6107 (1984).
- 2) C. E. D. Chidesey, C. R. Bertozzi, T. M. Putvinski, and A. M. Muijsce, *J. Am. Chem. Soc.*, **112**, 4301 (1990).
- 3) C. Miller, P. Cuendet, and M. Grötzel, *J. Phys. Chem.*, **95**, 877 (1991).
- 4) C. Miller and M. Grötzel, *J. Phys. Chem.*, **95**, 5225 (1991).
- 5) H. O. Finklea and D. D. Hanshaw, *J. Am. Chem. Soc.*, **114**, 3173 (1992).
- 6) N. J. Geddes, J. R. Sambles, D. J. Jarvis, and W. G. Parker, *Appl. Phys. Lett.*, **56**, 1916 (1990).
- 7) L. J. Kepley, R. M. Crooks, and A. J. Ricco, *Anal. Chem.*, **64**, 3191 (1992).
- 8) C. S. Dulcey, J. H. Georger, Jr., V. Krauthamer, D. A. Stenger, T. L. Fare, and J. M. Calvert, *Science*, **252**, 551 (1991).
- 9) A. Kumar, H. A. Biebuyck, N. L. Abbott, and G. M. Whitesides, *J. Am. Chem. Soc.*, **114**, 9188 (1992).
- 10) W. J. Dressick and J. M. Calvert, *Jpn. J. Appl. Phys., Part 1*, **32**, 5829 (1993).
- 11) L. Netzer and J. Sagiv, *J. Am. Chem. Soc.*, **105**, 674 (1983).
- 12) H. Lee, L. J. Kepley, H.-G. Hong, and T. E. Mallouk, *J. Am. Chem. Soc.*, **110**, 618 (1988).
- 13) H. Lee, L. J. Kepley, H.-G. Hong, S. Akhter, and T. E.

Mallouk, *J. Phys. Chem.*, **92**, 2597 (1988).

14) D. Li, M. A. Ratner, T. J. Marks, C.-H. Zhang, J. Yang, and G. K. Wong, *J. Am. Chem. Soc.*, **112**, 7389 (1990).

15) Y. Lvov, H. Haas, G. Decher, H. Möhwald, and A. Kalachev, *J. Phys. Chem.*, **97**, 12835 (1993).

16) Y. Lvov, F. Essler, and G. Decher, *J. Phys. Chem.*, **97**, 13773 (1993).

17) Y. Lvov, G. Decher, and G. Sukhorukov, *Macromolecules*, **26**, 5396 (1993).

18) J. Schmitt, T. Grunewald, K. Kjaer, P. Pershan, G. Decher, and M. Lösche, *Macromolecules*, **26**, 7058 (1993).

19) S. W. Keller, H.-N. Kim, and T. E. Mallouk, *J. Am. Chem. Soc.*, **116**, 8817 (1994).

20) H. E. Katz, G. Scheller, T. M. Putvinski, M. L. Schilling, W. L. Wilson, and C. E. D. Chidsey, *Science*, **254**, 1485 (1991).

21) S. D. Evans, A. Ulman, K. E. Goppert-Berarducci, and L. J. Gerenser, *J. Am. Chem. Soc.*, **113**, 5866 (1991).

22) S. B. Ungashe, W. L. Wilson, H. E. Katz, G. R. Schiller, and T. M. Putvinski, *J. Am. Chem. Soc.*, **114**, 8717 (1992).

23) Y. Umemura, K. -I. Tanaka, and A. Yamagishi, *J. Chem.*

Soc., Chem. Commun., **1992**, 67.

24) H. C. Yang, K. Aoki, H.-G. Hong, D. D. Sackett, M. F. Arendt, S.-L. Yau, C. M. Bell, and T. E. Mallouk, *J. Am. Chem. Soc.*, **115**, 11855 (1993).

25) A. C. Zeppenfeld, S. L. Fiddler, W. K. Ham, B. J. Klopfenstein, and C. J. Page, *J. Am. Chem. Soc.*, **116**, 9158 (1994).

26) C. M. Bell, M. F. Arendt, L. Gomez, R. H. Schmehl, and T. E. Mallouk, *J. Am. Chem. Soc.*, **116**, 8374 (1994).

27) H. Akhter, H. Lee, H.-G. Hong, T. E. Mallouk, and J. M. White, *J. Vac. Sci. Technol., A*, **7**, 1608 (1989).

28) G. Ertl and J. Kupperts, "Low Energy Electrons and Surface Chemistry," 2nd ed, VCH, Weinheim, FRG (1985), pp. 74–79.

29) M. B. Dines and P. M. DiGiacomo, *Inorg. Chem.*, **20**, 92 (1981).

30) C. D. Wagner, W. M. Riggs, L. E. Davis, J. F. Moulder, and G. E. Muilenberg, "Handbook of X-Ray Photoelectron Spectroscopy," ed by Perkin-Elmer Corporation, Physical Electronics Div., (1978).

31) H. Berthou and C. K. Jørgensen, *Anal. Chem.*, **47**, 482 (1975).